

Joint Power Control and Passive Beamforming in IRS-Assisted Spectrum Sharing

Xinrong Guan, *Member, IEEE*, Qingqing Wu, *Member, IEEE*, and Rui Zhang, *Fellow, IEEE*

Abstract—In cognitive radio (CR) communication systems, achieving high secondary user (SU) rate in the presence of strong cross-link interference with the primary user (PU) is a challenging problem. In this letter, we exploit the emerging intelligent reflecting surface (IRS) technology to tackle this problem. Specifically, we investigate an IRS-assisted CR communication system where an IRS is deployed to assist in the spectrum sharing between a PU link and an SU link. We aim to maximize the achievable SU rate subject to a given signal-to-interference-plus-noise ratio target for the PU link, by jointly optimizing the SU transmit power and IRS reflect beamforming. Since the formulated problem is difficult to solve due to its non-convexity and coupled variables, we propose an efficient algorithm based on alternating optimization and successive convex approximation techniques to solve it sub-optimally, along with some heuristic designs for lower complexity. Simulation results show that IRS is able to significantly improve the SU rate, even for the scenarios deemed most challenging in conventional CR systems without using IRS.

Index Terms—intelligent reflecting surface, spectrum sharing, power control, passive beamforming

I. INTRODUCTION

Due to the ever increasing demand for higher data rates and tremendous growth in the number of communication devices, a variety of wireless technologies have been proposed, such as massive multiple-input multiple-output (MIMO), millimeter wave (mmWave) communications, etc. However, to implement such technologies in practical systems, the increased network energy consumption and hardware cost become critical issues. Recently, intelligent reflecting surface (IRS) has emerged as a promising technology to achieve high spectrum and energy efficiency for wireless communication cost-effectively [1]–[5]. Specifically, IRS is a uniform planar array consisting of a large number of passive reflecting elements. By adaptively adjusting the reflection coefficient of each element, the reflected signal by IRS can be added constructively/destructively with those via other propagation paths to enhance/suppress the received signal in desired directions. As a result, IRS passive beamforming has been incorporated into various wireless systems such as orthogonal frequency division multiplexing (OFDM) [6]–[8], simultaneous wireless information and power transfer (SWIPT) [9,10] and secrecy communication [11]–[14], non-orthogonal multiple access (NOMA) [15]–[17], etc. In particular, artificial noise is used to improve the achievable secrecy rate in [11]

On the other hand, cognitive radio (CR) has been thoroughly investigated in the literature to solve the spectrum scarcity problem in wireless communication [18]. By allowing secondary users (SUs) to share the spectrum with primary users (PUs) provided their quality of service (QoS) is ensured, the spectrum efficiency of their co-existing system can be significantly improved. However, in scenarios when the SU is located nearby the PU, e.g., they are in the same hotspot, the achievable SU rate becomes very limited due to the strong cross-link interference with the PU. For instance, in a CR communication system shown in Fig. 1 (ignoring the IRS for the time being), the PU named P1 and the SU named S1 are located near each other, intending to communicate with their partners, i.e., the PU named P2 and the SU named S2, respectively. In practice, P1 and P2 can be, e.g., a mobile terminal and its serving access point/base station, whereas S1 and S2 may be a device-to-device (D2D) communication pair or Internet of Things (IoT) devices aiming to share the spectrum of the PU link for opportunistic communication. Considering each of the PU and SU nodes as a transmitter or receiver, four different communication scenarios are shown in Fig. 1. In Fig. 1(a) and Fig. 1(b), the cross interfering links are symmetric, i.e. the interference from the primary transmitter (PT) to the secondary receiver (SR) is comparable to that from the secondary transmitter (ST) to the primary receiver (PR). While in the asymmetric interference scenarios Fig. 1(c) and Fig. 1(d), the interference in one of the two cross links is much stronger than that in the other. Apparently, the asymmetric interference scenario is more challenging for SU to achieve high data rate. An effective approach for the scenario Fig. 1(c) is to apply the successive interference cancellation (SIC) at the SR so that the strong primary interference can be first decoded and then removed from the received signal. However, this method requires the knowledge of the codebook used by the PU and cannot deal with the most challenging scenario Fig. 1(d) where the strong interference from the ST to the PR is the performance bottleneck since the PR is not supposed to apply SIC in typical CR setups [18].

By exploiting its passive beamforming for signal enhancement as well as interference suppression, IRS is potentially a promising solution to tackle the above CR challenges. This thus motivates the current work to investigate the joint ST power control and IRS reflection optimization in an IRS-assisted CR communication system shown in Fig. 1. We aim to maximize the achievable SU rate of the considered system subject to a target QoS for the PU, and investigate how IRS helps resolve the aforementioned strong interference issue, which, has not been addressed in the literature yet.

X. Guan is with the College of Communications Engineering, Army Engineering University of PLA, Nanjing, 210007, China (e-mail: geniusg2017@gmail.com). Q. Wu and R. Zhang are with the Department of Electrical and Computer Engineering, National University of Singapore, 117583, Singapore (e-mails: elewuqq, elezhang@nus.edu.sg).

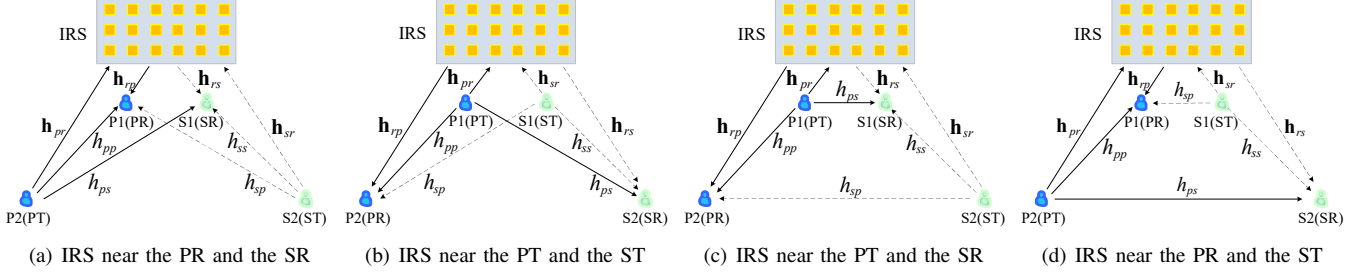


Fig. 1: IRS-assisted CR communication system subjected to (a)/(b) symmetric and (c)/(d) asymmetric interference.

II. SYSTEM MODEL AND PROBLEM FORMULATION

A. System Model

As shown in Fig. 1, we consider an IRS-assisted CR/spectrum sharing system, where an SU link consisting of S1 and S2 coexists with a PU link consisting of P1 and P2, and an IRS is deployed nearby P1 and S1 to enable a communication hotspot. Assume that all nodes are equipped with a single antenna, while the number of reflecting elements at the IRS is denoted by N . The baseband equivalent channels from the PT(ST) to the PR, the SR and the IRS are denoted by \mathbf{h}_{pp} , \mathbf{h}_{ps} and $\mathbf{h}_{pr}^H \in \mathbb{C}^{1 \times N}$ (\mathbf{h}_{sp} , \mathbf{h}_{ss} and $\mathbf{h}_{sr}^H \in \mathbb{C}^{1 \times N}$), respectively, while those from the IRS to the PR and the SR are denoted by $\mathbf{h}_{rp}^H \in \mathbb{C}^{1 \times N}$ and $\mathbf{h}_{rs}^H \in \mathbb{C}^{1 \times N}$, respectively. Let $\Phi = \text{diag}(v_1, v_2, \dots, v_N)$ represent the diagonal phase-shifting matrix of the IRS [1], where $v_n = e^{j\theta_n}$ and $\theta_n \in [0, 2\pi)$ is the phase shift on the combined incident signal by its n -th element, $n=1, \dots, N$. The composite PT/ST-IRS-PR/SR channel is then modeled as a concatenation of three components, namely, the PT/ST-IRS link, the IRS reflecting with phase shifts, and the IRS-PR/SR link. The quasi-static flat-fading model is assumed for all channels. Based on the various channel acquisition methods discussed in [1], we assume that the channel state information (CSI) of all channels involved is perfectly known at the ST/IRS for the joint power control and passive beamforming design. Though the assumption of perfect CSI knowledge is ideal, the result obtained in this letter provides useful insights and performance bounds for practical systems with partial/imperfect CSI, which need further investigation in future work. Note that it is reasonable to assume that the CSI of P1-P2 link is known since PUs are motivated to share the CSI with the SUs/IRS for guaranteeing the QoS of the primary transmission.

Assume that the transmitted signals from the PT and the ST are given by $x_p \sim \mathcal{CN}(0, 1)$ and $x_s \sim \mathcal{CN}(0, 1)$, respectively. The transmit power of the PT is fixed as $p_p = P_0$, whereas that of the ST can be varied, subject to a maximum power budget denoted by $p_s \leq P_{\max}$. As a result, the received signals at the PR and the SR are respectively given by

$$y_p = \sqrt{p_p} (\mathbf{h}_{pp} + \mathbf{h}_{rp}^H \Phi \mathbf{h}_{pr}^*) x_p + \sqrt{p_s} (\mathbf{h}_{sp} + \mathbf{h}_{rp}^H \Phi \mathbf{h}_{sr}^*) x_s + n_p, \quad (1)$$

$$y_s = \sqrt{p_s} (\mathbf{h}_{ss} + \mathbf{h}_{rs}^H \Phi \mathbf{h}_{sr}^*) x_s + \sqrt{p_p} (\mathbf{h}_{ps} + \mathbf{h}_{rs}^H \Phi \mathbf{h}_{pr}^*) x_p + n_s, \quad (2)$$

where $n_p \sim \mathcal{CN}(0, \sigma_p^2)$ and $n_s \sim \mathcal{CN}(0, \sigma_s^2)$ denote the complex additive white Gaussian noise (AWGN) at the PR and the SR, respectively. Denoting $\mathbf{h}_{irj} = \text{diag}(\mathbf{h}_{irj}^H) \mathbf{h}_{irj}^*$ and $\mathbf{v}^H =$

$[v_1, v_2, \dots, v_N]$, we have $\mathbf{h}_{rj}^H \Phi \mathbf{h}_{ir}^* = \mathbf{v}^H \mathbf{h}_{irj}$, $i, j \in \{p, s\}$. Thus, the signal-to-interference-plus-noise ratio (SINR) at the PR and the SR can be respectively expressed as

$$\gamma_p = \frac{p_p |\mathbf{v}^H \mathbf{h}_{prp} + \mathbf{h}_{pp}|^2}{p_s |\mathbf{v}^H \mathbf{h}_{srp} + \mathbf{h}_{sp}|^2 + \sigma_p^2}, \quad (3)$$

$$\gamma_s = \frac{p_s |\mathbf{v}^H \mathbf{h}_{sr s} + \mathbf{h}_{ss}|^2}{p_p |\mathbf{v}^H \mathbf{h}_{prs} + \mathbf{h}_{ps}|^2 + \sigma_s^2}. \quad (4)$$

To guarantee the QoS of the PU link, we impose the SINR constraint at PR as $\gamma_p \geq \gamma_{\text{th}}$, where γ_{th} is the PU SINR target.

B. Problem Formulation

We aim to maximize the achievable SU rate $R_s = \log_2(1 + \gamma_s)$ in bits/second/Hertz (bps/Hz) via joint the power control at the ST with the reflect beamforming at the IRS, subject to the SINR constraint at the PR. Thus, the optimization problem is formulated as

$$\begin{aligned} \text{(P0)} : \max_{p_s, \mathbf{v}} \quad & \log_2 \left(1 + \frac{p_s |\mathbf{v}^H \mathbf{h}_{sr s} + \mathbf{h}_{ss}|^2}{p_p |\mathbf{v}^H \mathbf{h}_{prs} + \mathbf{h}_{ps}|^2 + \sigma_s^2} \right) \\ \text{s.t.} \quad & \frac{p_p |\mathbf{v}^H \mathbf{h}_{prp} + \mathbf{h}_{pp}|^2}{p_s |\mathbf{v}^H \mathbf{h}_{srp} + \mathbf{h}_{sp}|^2 + \sigma_p^2} \geq \gamma_{\text{th}}, \\ & p_s \leq P_{\max}, \\ & |v_n| = 1, n = 1, \dots, N. \end{aligned}$$

(P0) is difficult to solve due to the non-concave objective function as well as the coupled optimization variables. However, we observe that when one of p_s and \mathbf{v} is fixed, the resultant problems can be efficiently solved. This thus motivates us to propose an alternating optimization (AO) based algorithm to solve (P0) sub-optimally, by iteratively optimizing one of p_s and \mathbf{v} with the other being fixed at each iteration until the convergence is reached.

III. PROPOSED SOLUTIONS

In this section, we propose the AO based algorithm first, followed by some heuristic designs for reducing the complexity.

A. Alternating Optimization Based Joint Design

1) *Optimizing p_s for Given \mathbf{v}* : Denoting $\bar{\mathbf{h}}_{ij} = [\mathbf{h}_{irj}^T \ \mathbf{h}_{ij}^T]^T$ and $\tilde{\mathbf{v}}^H = e^{j\varpi} [\mathbf{v}^H \ 1]$ where ϖ is an arbitrary phase rotation, then the equivalent channel power gain is given by $\alpha_{ij} = |\tilde{\mathbf{v}}^H \bar{\mathbf{h}}_{ij}|^2$, $i, j \in \{s, p\}$. Thus, (P0) can be rewritten as

$$\begin{aligned} \text{(P1)} : \max_{p_s} \quad & \log_2 \left(1 + \frac{p_s \alpha_{ss}}{p_p \alpha_{ps} + \sigma_s^2} \right) \\ \text{s.t.} \quad & \frac{p_p \alpha_{pp}}{p_s \alpha_{sp} + \sigma_p^2} \geq \gamma_{\text{th}}, \\ & p_s \leq P_{\max}. \end{aligned}$$

It can be observed that the objective function in (P1) is a

Algorithm 1: Alternating optimization for solving (P0)**Input:** $N, P_{\max}, \sigma_j^2, \gamma_{\text{th}}, h_{irj}, h_{ij}, i, j \in \{p, s\}$.**Output:** p_s, \mathbf{v} .

- 1 Initialize the phase-shift vector as $\boldsymbol{\theta}^{(0)} = [\theta_1, \dots, \theta_N]^T$.
- 2 Set $l = 1$, $\mathbf{v}^{(0)} = [e^{j\theta_1}, \dots, e^{j\theta_N}]^T$ and $\tilde{\mathbf{v}}^{(0)} = \begin{bmatrix} \mathbf{v}^{(0)} \\ 1 \end{bmatrix}$.
- 3 **repeat**
- 4 For given $\tilde{\mathbf{v}}^{(l-1)}$, obtain $p_s^{(l)}$ according to (5).
- 5 For given $p_s^{(l)}$, update \mathbf{A}_{jj} and \mathbf{B}_{ij} . Set $\tilde{\mathbf{v}}_0 = \tilde{\mathbf{v}}^{(l-1)}$ and update $\mathbf{w}_{ss}^H, \mathbf{w}_{pp}^H, d_{ss}$ and d_{pp} according to (8) and (9).
- 6 **repeat**
- 7 If $\gamma_p(0) \geq \gamma_{\text{th}}$, $u_n^* = e^{j\angle(w_{ss}(n))}$. Otherwise, solve λ^* via bisection search and obtain \mathbf{u}^* in (12).
- 8 Update $\tilde{\mathbf{v}}_0$ as $\tilde{\mathbf{v}}_0 = \mathbf{u}^*$ and $\mathbf{w}_{ss}^H, \mathbf{w}_{pp}^H, d_{ss}$ and d_{pp} according to (8) and (9).
- 9 **until** the objective value in (P2.3) reaches convergence.
- 10 Update $\tilde{\mathbf{v}}^{(l)} = \mathbf{u}^*$ and $l = l + 1$.
- 11 **until** the objective value in (P0) reaches convergence.
- 12 Obtain \mathbf{v} from $\tilde{\mathbf{v}}$ according to (13).

monotonically increasing function of p_s , thus the optimal p_s can be obtained in closed-form as

$$p_s^* = \max(0, \min((P_0 \alpha_{pp} / \gamma_{\text{th}} - \sigma_p^2) / \alpha_{sp}, P_{\max})). \quad (5)$$

2) *Optimizing \mathbf{v} for Given p_s :* For given p_s , denoting $\mathbf{H}_{ij} = \mathbf{h}_{ij} \mathbf{h}_{ij}^H$, $\mathbf{A}_{jj} = p_j \mathbf{H}_{jj}$ and $\mathbf{B}_{ij} = p_i \mathbf{H}_{ij} + \mathbf{I}_{N+1} \sigma_j^2 / (N+1)$, where $i, j \in \{p, s\}$ and \mathbf{I}_N is the $N \times N$ identity matrix, then (P0) can be reformulated as

$$\begin{aligned} \text{(P2.1)} : \max_{\tilde{\mathbf{v}}} & \frac{\tilde{\mathbf{v}}^H \mathbf{A}_{ss} \tilde{\mathbf{v}}}{\tilde{\mathbf{v}}^H \mathbf{B}_{ps} \tilde{\mathbf{v}}} \\ \text{s.t.} & \frac{\tilde{\mathbf{v}}^H \mathbf{A}_{pp} \tilde{\mathbf{v}}}{\tilde{\mathbf{v}}^H \mathbf{B}_{sp} \tilde{\mathbf{v}}} \geq \gamma_{\text{th}}, \\ & |\tilde{v}_n| = 1, n = 1, \dots, N+1. \end{aligned} \quad (6.1) \quad (6.2)$$

However, (P2.1) is still difficult to solve since it is a fractional quadratically constrained quadratic programming (QCQP) problem with unit modulus constraints. To overcome such difficulty, we apply the successive convex approximation (SCA) technique to transform (P2.1) into a series of more tractable approximated subproblems. In particular, we resort to the following lemma to derive a lower bound on the objective function and the left-hand-side (LHS) of (6.1), respectively.

Lemma 1. Denoting $f(\mathbf{A}_{jj}, \mathbf{B}_{ij}, \tilde{\mathbf{v}}) = \frac{\tilde{\mathbf{v}}^H \mathbf{A}_{jj} \tilde{\mathbf{v}}}{\tilde{\mathbf{v}}^H \mathbf{B}_{ij} \tilde{\mathbf{v}}}$, $i, j \in \{p, s\}$, $i \neq j$, then the following inequality holds for any given $\tilde{\mathbf{v}}_0$,

$$f(\mathbf{A}_{jj}, \mathbf{B}_{ij}, \tilde{\mathbf{v}}) \geq 2\text{Re}\{\mathbf{w}_{ij}^H \tilde{\mathbf{v}}\} + d_{jj}, \quad (7)$$

where

$$\mathbf{w}_{jj}^H = \frac{\tilde{\mathbf{v}}_0^H \mathbf{A}_{jj}}{\tilde{\mathbf{v}}_0^H \mathbf{B}_{ij} \tilde{\mathbf{v}}_0} - \tilde{\mathbf{v}}_0^H (\mathbf{B}_{ij} - \lambda_{\mathbf{B}_{ij}} \mathbf{I}_{N+1}) \frac{\tilde{\mathbf{v}}_0^H \mathbf{A}_{jj} \tilde{\mathbf{v}}_0}{(\tilde{\mathbf{v}}_0^H \mathbf{B}_{ij} \tilde{\mathbf{v}}_0)^2}, \quad (8)$$

$$d_{jj} = -\left[2\lambda_{\mathbf{B}_{ij}}(N+1) - \tilde{\mathbf{v}}_0^H \mathbf{B}_{ij} \tilde{\mathbf{v}}_0\right] \frac{\tilde{\mathbf{v}}_0^H \mathbf{A}_{jj} \tilde{\mathbf{v}}_0}{(\tilde{\mathbf{v}}_0^H \mathbf{B}_{ij} \tilde{\mathbf{v}}_0)^2}, \quad (9)$$

and $\lambda_{\mathbf{B}_{ij}}$ denotes the maximum eigenvalue of \mathbf{B}_{ij} .

Proof: See Appendix A. \square

According to **Lemma 1**, we have $\frac{\tilde{\mathbf{v}}^H \mathbf{A}_{ss} \tilde{\mathbf{v}}}{\tilde{\mathbf{v}}^H \mathbf{B}_{ps} \tilde{\mathbf{v}}} \geq 2\text{Re}\{\mathbf{w}_{ss}^H \tilde{\mathbf{v}}\} + d_{ss}$ and $\frac{\tilde{\mathbf{v}}^H \mathbf{A}_{pp} \tilde{\mathbf{v}}}{\tilde{\mathbf{v}}^H \mathbf{B}_{sp} \tilde{\mathbf{v}}} \geq 2\text{Re}\{\mathbf{w}_{pp}^H \tilde{\mathbf{v}}\} + d_{pp}$. Then, we consider the following optimization problem for given $\tilde{\mathbf{v}}_0$,

$$\begin{aligned} \text{(P2.2)} : \max_{\tilde{\mathbf{v}}} & 2\text{Re}\{\mathbf{w}_{ss}^H \tilde{\mathbf{v}}\} + d_{ss} \\ \text{s.t.} & 2\text{Re}\{\mathbf{w}_{pp}^H \tilde{\mathbf{v}}\} + d_{pp} \geq \gamma_{\text{th}}, \\ & |\tilde{v}_n| = 1, n = 1, \dots, N+1. \end{aligned}$$

The remaining difficulty in solving (P2.2) lies in the non-convexity of the unit modulus constraints. In the following, we first construct a convex problem (P2.3) which is obtained by properly relaxing the non-convex constraints in (P2.2), then show that the optimal solution to (P2.3) must satisfy the unit modulus constraints and thus is also optimal to (P2.2).

$$\begin{aligned} \text{(P2.3)} : \max_{\mathbf{u}} & 2\text{Re}\{\mathbf{w}_{ss}^H \mathbf{u}\} + d_{ss} \\ \text{s.t.} & 2\text{Re}\{\mathbf{w}_{pp}^H \mathbf{u}\} + d_{pp} \geq \gamma_{\text{th}}, \end{aligned} \quad (10.1)$$

$$|u_n|^2 \leq 1, n = 1, \dots, N+1. \quad (10.2)$$

Denoting the dual variables associated with constraints (10.1) and (10.2) by $\lambda \geq 0$ and $\mu_n \geq 0$, $n=1, \dots, N+1$, respectively, and the n -th element in \mathbf{w}_{ss} and \mathbf{w}_{pp} by $w_{ss}(n)$ and $w_{pp}(n)$, respectively. A closed-form expression for the optimal solution to (P2.3) is given by the following proposition.

Proposition 1. The optimal solution to (P2.3) is $u_n^* = e^{j\angle(w_{ss}(n) + \lambda w_{pp}(n))}$, where $\angle(x)$ denotes the phase of x .

Proof: See Appendix B. \square

Based on **Proposition 1**, we have $u_n^* = e^{j\angle(w_{ss}(n))}$, $\forall \lambda \geq 0$, if $\angle(w_{ss}(n)) = \angle(w_{pp}(n))$. Otherwise, we consider the following two cases to derive the optimal λ , denoted by λ^* . Rewrite the LHS of (10.1) as

$$\gamma_p(\lambda) = 2 \sum_n \text{Re}\{w_{pp}^*(n) e^{j\angle(w_{ss}(n) + \lambda w_{pp}(n))}\} + d_{pp}. \quad (11)$$

Case (1): Assume that $\lambda^* = 0$, then u_n^* is rewritten as $u_n^* = e^{j\angle(w_{ss}(n))}$, which has to satisfy the SINR constraint in (10.1), i.e. $\gamma_p(0) \geq \gamma_{\text{th}}$ must hold. Otherwise, it should be Case (2).

Case (2): $\lambda^* > 0$, then it follows that the equality $\gamma_p(\lambda^*) = \gamma_{\text{th}}$ must hold according to the complementary slackness condition. To find λ^* satisfying $\gamma_p(\lambda^*) = \gamma_{\text{th}}$, we provide the following lemma.

Lemma 2. $\gamma_p(\lambda)$ is a monotonically increasing function of λ if $\angle(w_{ss}(n)) \neq \angle(w_{pp}(n))$.

Proof: See Appendix C. \square

Based on **Lemma 2**, if $\gamma_p(\infty) < \gamma_{\text{th}}$, $\gamma_p(\lambda^*) = \gamma_{\text{th}}$ is infeasible and so is problem (P2.3). Otherwise, λ^* can be obtained by using the bisection search method. After λ^* is obtained, u_n^* in Case (2) is given by

$$u_n^* = e^{j\angle(w_{ss}(n) + \lambda^* w_{pp}(n))}, n = 1, \dots, N+1. \quad (12)$$

Note that \mathbf{u}^* is optimal to (P2.3) and satisfies all the constraints in (P2.2), thus $\tilde{\mathbf{v}}^* = \mathbf{u}^*$ is the optimal solution to (P2.2). Otherwise, it implies that there exists a feasible solution to (P2.2) (also feasible to (P2.3)) that achieves a larger objective value than the optimal objective value of (P2.3) achieved by \mathbf{u}^* , which causes contradiction. As such, an approximate solution to (P2.1) is obtained by successively solving (P2.3) and updating $\tilde{\mathbf{v}}_0$ as $\tilde{\mathbf{v}}_0 = \mathbf{u}^*$. Finally, the reflection coefficients are obtained as

$$v_n^* = e^{j\angle(\tilde{v}_n^* / \tilde{v}_{N+1}^*)}, n = 1, \dots, N. \quad (13)$$

3) *Overall Algorithm:* To summarize, the overall iterative algorithm to solve (P0) is given in Algorithm 1. The main complexity of Algorithm 1 is due to computing $\mathbf{w}_{ss}^H, \mathbf{w}_{pp}^H, d_{ss}$ and d_{pp} in Step 5 and Step 8. Specifically, denoting the number of iterations required for the objective value of (P2.3) and (P0) to reach convergence by L_1 and L_2 , respectively, the overall complexity is obtained as $\mathcal{O}(L_2(L_1 + 1)(N + 1)^3)$.

B. Low Complexity Two-Stage Designs

Next, low complexity two-stage designs are proposed to reduce the implementation overhead. Specifically, in the first stage, the passive beamforming is optimized to maximize the channel power gain of the equivalent PT-PR/ST-SR (desired) link, i.e. α_{pp} and α_{ss} , respectively, or to minimize that of the equivalent PT-SR/ST-PR (interference) link, i.e. α_{ps} and α_{sp} , respectively. In the second stage, the transmit power at the ST is optimized similarly as (5). The passive beamforming vector design in the first stage is specified as follows.

1) *Signal power maximization based designs:* Assuming that \mathbf{v} is designed to maximize α_{pp} , the optimization problem is formulated as

$$\begin{aligned} (\text{P3}) : \max_{\mathbf{v}} & \quad \left| \mathbf{v}^H \mathbf{h}_{prp} + h_{pp} \right|^2 \\ \text{s.t.} & \quad |v_n| = 1, n = 1, \dots, N. \end{aligned}$$

The optimal solution is given by [3]

$$v_n^* = e^{j(\angle h_{pp} - \angle h_{prp}(n))}, n = 1, \dots, N. \quad (14)$$

Similarly, the optimal \mathbf{v} maximizing α_{ss} can be obtained.

2) *Interference power minimization based designs:* First, design \mathbf{v} to minimize α_{sp} , which is formulated as

$$\begin{aligned} (\text{P4}) : \min_{\mathbf{v}} & \quad \left| \mathbf{v}^H \mathbf{h}_{srp} + h_{sp} \right|^2 \\ \text{s.t.} & \quad |v_n| = 1, n = 1, \dots, N. \end{aligned}$$

Case (1): If $\sum_n |h_{srp}(n)| \leq |h_{sp}|$, which implies that the maximum channel power gain of the reflecting ST-IRS-PR link is no larger than that of the direct ST-PR link, then we have $\min_{\mathbf{v}} \alpha_{sp} = (|h_{sp}| - \sum_n |h_{srp}(n)|)^2$. This suggests that the interference cannot be completely canceled in this case. The optimal reflection coefficients are thus given by

$$v_n^* = e^{j(\pi + \angle h_{sp} - \angle h_{srp}(n))}, n = 1, \dots, N. \quad (15)$$

Case (2): If $\sum_n |h_{srp}(n)| > |h_{sp}|$, define a matrix as $\tilde{\mathbf{V}} = \tilde{\mathbf{v}}\tilde{\mathbf{v}}^H$, then it follows that $\tilde{\mathbf{V}} \succeq 0$ and $\text{rank}(\tilde{\mathbf{V}}) = 1$. By applying the semidefinite relaxation (SDR) to relax the non-convex rank-1 constraint, (P4) is reduced to

$$\begin{aligned} (\text{P4.1}) : \min_{\tilde{\mathbf{V}}} & \quad \text{Tr}(\mathbf{H}_{sp} \tilde{\mathbf{V}}) \\ \text{s.t.} & \quad \tilde{\mathbf{V}}_{n,n} = 1, n = 1, \dots, N+1, \end{aligned}$$

where \mathbf{H}_{sp} is given in Section III-A-2). (P4.1) can be efficiently solved by using a convex optimization solver. If the obtained $\tilde{\mathbf{V}}$ is of rank-1, the optimal reflection coefficients can be obtained by applying eigenvalue decomposition as $\tilde{\mathbf{V}} = \tilde{\mathbf{v}}\tilde{\mathbf{v}}^H$. Otherwise, the suboptimal solution can be recovered from $\tilde{\mathbf{V}}$ via Gaussian randomization [3]. Similarly, the optimal/suboptimal \mathbf{v} minimizing α_{ps} can be obtained.

IV. SIMULATION RESULTS

To study the effect of IRS on the CR communication system, we consider three different setups, namely Setup (1), (2) and (3), corresponding to the scenarios Fig. 1(a), (c) and (d), respectively. Note that the scenario Fig. 1(b) is omitted since its result is similar to that of Fig. 1(a). The deployment of P1, P2, S1, S2 and IRS is illustrated in Fig. 2. We assume that the system operates on a carrier frequency of 750 MHz with the wavelength $\lambda_c = 0.4$ m and the path loss at the reference distance $d_0 = 1$ m is given by $L_0 = -30$ dB. Suppose that the IRS is equipped with a uniform planar array with 6 rows and 10 columns, and the element spacing is $\Delta d = 3\lambda_c/8$. The

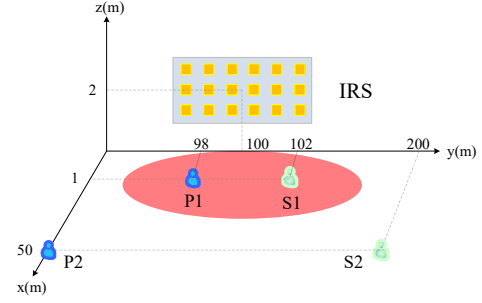


Fig. 2: Simulation setup.

noise power is set as $\sigma_p^2 = \sigma_s^2 = -105$ dBm. The channel between P1 and P2 is generated by $h_{pp}^H = (L_0 D_{pp}^{-c_{pp}})^{1/2} g_{pp}$, where D_{pp} denotes the distance from P1 to P2 and c_{pp} denotes the corresponding path loss exponent. The small-scale fading component g_{pp} is assumed to be Rician fading and given by $g_{pp} = \sqrt{\beta_{pp}/(1+\beta_{pp})} g_{pp}^{\text{LoS}} + \sqrt{1/(1+\beta_{pp})} g_{pp}^{\text{NLoS}}$, where β_{pp} is the Rician factor, g_{pp}^{LoS} and g_{pp}^{NLoS} represent the deterministic line-of-sight (LoS) and Rayleigh fading/non-LoS (NLoS) components, respectively. The same channel model is adopted for all other channels in general. In particular, we assume that the channels among the ground nodes, i.e. P1, S1, P2 and S2, as well as those between IRS and P2/S2 have no LoS component due to terrestrial rich scattering/Rayleigh fading with the path loss exponents and Rician factors set as 3 and 0, respectively, whereas the channels between IRS and P1/S1 are LoS due to the higher altitude of the IRS and its short distances with P1/S1, with the path loss exponents and Rician factors set as 2 and ∞ , respectively.

Besides the proposed AO based design (IRS, AO) and four low-complexity designs (IRS, max α_{pp}), (IRS, max α_{ss}), (IRS, min α_{sp}) and (IRS, min α_{ps}), the cases without IRS and with/without SIC at the SR, i.e. (no-IRS, w/ SIC) and (no-IRS, w/o SIC), are also considered for performance comparison and showing the benefit of using IRS.

Fig. 3 shows the achievable SU rate versus the maximum transmit power of the ST in the three setups. In Setup (1), the SU rate for the cases of (no-IRS, w/ SIC) and (IRS, min α_{ps}) remains unchanged when $P_{\max} \geq 20$ dBm, whereas those for the cases of (IRS, AO) and (IRS, min α_{sp}) can sustain increasing with P_{\max} . This is because in the cases of (no-IRS, w/ SIC) and (IRS, min α_{ps}), though the interference from the PT(P2) to the SR(S1) is mitigated, p_s is still restricted by the maximum tolerable interference at the PR(P1) and thus the SU rate becomes saturated. While in the cases of (IRS, AO) and (IRS, min α_{sp}), the interference from the ST(S2) to the PR(P1) is reduced/minimized by IRS reflection, which thus allows the ST(S2) to increase its transmit power for achieving higher SU rate. One can also observe that all low-complexity designs incur substantial rate loss as compared to the AO based one. This implies that in Setup (1), the benefit of using IRS is manifold, rather than solely enhancing or weakening any single signal/interference link.

In Setup (2), the case of (IRS, AO) always achieves higher SU rate than that of (no-IRS, w/ SIC). The reason is that using IRS not only cancels the interference from the PT(P1) to the SR(S1), but also enhances the desired signal from the ST(S2) to the SR(S1). It is also observed that the case of (IRS, min

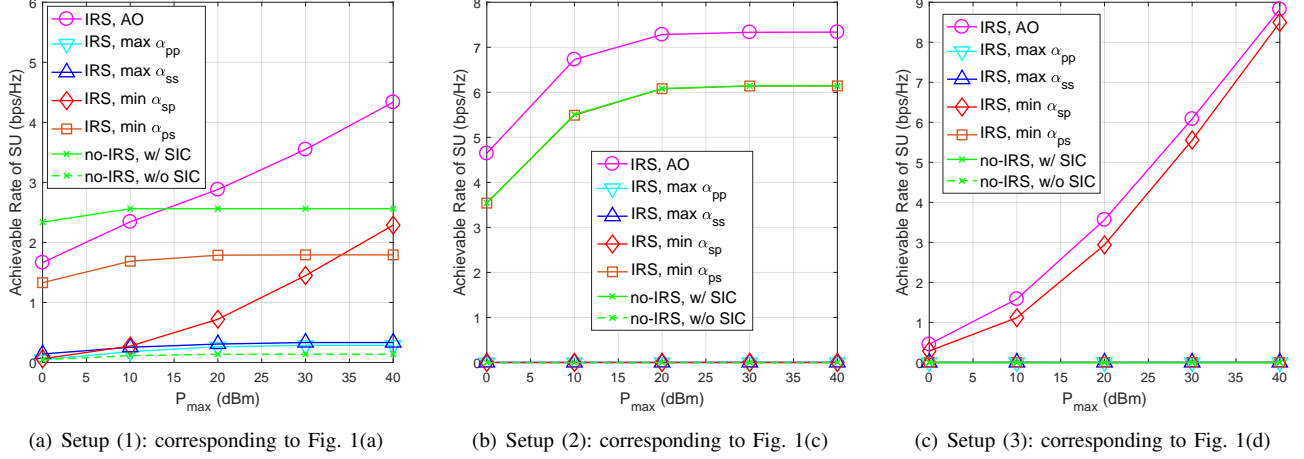


Fig. 3: Achievable SU rate for different IRS beamforming designs, with $N=60$, $P_0=20$ dBm, and $\gamma_{th}=20$ dB.

α_{ps}) achieves nearly the same SU rate as that of (no-IRS, w/ SIC), which implies that when both the PT(P1) and the SR(S1) are nearby the IRS, the low-complexity design minimizing α_{ps} cancels the interference from the PT(P1) to the SR(S1) effectively. However, the other three low-complexity designs are all ineffective for dealing with this strong interference scenario and thus the achievable SU rate is 0. Moreover, note that the SU rate for the case of (IRS, AO) eventually saturates. This is because both the ST(S2) and the PR(P2) are not in the coverage of IRS and thus the interference from the ST(S2) to the PR(P2) cannot be reduced.

Finally, for Setup (3), both no-IRS designs are ineffective, regardless of whether SIC is applied at the SR(S2) or not. This is expected since given the severe interference from the ST(S1) to the PR(P1), the former should keep silent to guarantee the QoS of the latter. This is also the most challenging scenario in conventional CR systems without using IRS. While with our proposed designs (IRS, AO) and (IRS, min α_{sp}), such interference is reduced by IRS reflection, thus the SU can access the spectrum and achieve higher rate with increased transmit power. Moreover, similar to no-IRS designs, the other three low-complexity designs are also ineffective because none of them can handle the severe ST-PR interference in this setup.

V. CONCLUSION

In this letter, we formulated the SU rate maximization problem for the joint power control with IRS reflect beamforming. We developed an AO based algorithm to solve the design problem efficiently and showed by simulations the effectiveness of exploiting IRS to improve SU rate and its advantages in dealing with some challenging interference scenarios in conventional CR systems without using IRS.

APPENDIX A

Consider the function $f(x, y) = |x|^2/y$, $x \in \mathbb{C}$, $y \in \mathbb{R}^{++}$. Since $f(x, y)$ is jointly convex w.r.t. (x, y) , applying the first-order Taylor expansion at (x_0, y_0) yields

$$f(x, y) \geq 2\text{Re}\{x_0^*x\}/y_0 - |x|^2/y_0^2. \quad (16)$$

Setting $x = \tilde{\mathbf{h}}_{ss}^H \tilde{\mathbf{v}}$, $x_0 = \tilde{\mathbf{h}}_{ss}^H \tilde{\mathbf{v}}_0$, $y = \tilde{\mathbf{v}}^H \mathbf{B}_{ps} \tilde{\mathbf{v}}$ and $y_0 = \tilde{\mathbf{v}}_0^H \mathbf{B}_{ps} \tilde{\mathbf{v}}_0$, we have

$$f(\mathbf{A}_{ss}, \mathbf{B}_{ps}, \tilde{\mathbf{v}}) \geq \frac{2\text{Re}\{\tilde{\mathbf{v}}_0^H \mathbf{A}_{ss} \tilde{\mathbf{v}}\}}{\tilde{\mathbf{v}}_0^H \mathbf{B}_{ps} \tilde{\mathbf{v}}_0} - \frac{\tilde{\mathbf{v}}_0^H \mathbf{A}_{ss} \tilde{\mathbf{v}}_0}{(\tilde{\mathbf{v}}_0^H \mathbf{B}_{ps} \tilde{\mathbf{v}}_0)^2} \tilde{\mathbf{v}}^H \mathbf{B} \tilde{\mathbf{v}}. \quad (17)$$

By applying Lemma 1 in [19], an upper bound on $\tilde{\mathbf{v}}^H \mathbf{B} \tilde{\mathbf{v}}$ is given by

$$\tilde{\mathbf{v}}^H \mathbf{B} \tilde{\mathbf{v}} \leq 2\text{Re}\{\tilde{\mathbf{v}}_0^H (\mathbf{B}_{ps} - \lambda \mathbf{B}_{ps} \mathbf{I}_{N+1}) \tilde{\mathbf{v}}\} + 2\lambda \mathbf{B}_{ps} (N+1) - \tilde{\mathbf{v}}_0^H \mathbf{B}_{ps} \tilde{\mathbf{v}}_0.$$

Substituting it into (17), we obtain (7).

APPENDIX B

The Lagrangian associated with (P2.3) is expressed as

$$L(\mathbf{u}, \lambda, \{\mu_n\}) = \sum_n (2\text{Re}\{\tilde{\mathbf{v}}_0^H (w_{ss}^*(n) + \lambda w_{pp}^*(n)) u_n\} - \mu_n |u_n|^2) + \sum_n \mu_n + d_{ss} + \lambda d_{pp} - \lambda \gamma_{th}. \quad (18)$$

Accordingly, the dual function is given by $g(\lambda, \{\mu_n\}) = \sup_{\mathbf{u}} L(\mathbf{u}, \lambda, \{\mu_n\})$. To make $g(\lambda, \{\mu_n\})$ bounded from above, i.e., $g(\lambda, \{\mu_n\}) < \infty$, it follows that $\mu_n > 0$, $\forall n$, must hold. Denoting the optimal primal and dual variables by \mathbf{u}^* , λ^* and μ_n^* , $\forall n$, then \mathbf{u}^* , λ^* and μ_n^* should satisfy the Karush-Kuhn-Tucker (KKT) optimality conditions. Using the complementary slackness condition for (10.2), we have $\mu_n^* (1 - |u_n^*|^2) = 0$. Since $\mu_n^* > 0$ always holds, u_n^* has to satisfy $|u_n^*| = 1$. By exploiting the first-order optimality condition to maximize the Lagrangian in (18), u_n^* with fixed λ and μ_n is derived as $u_n^* = (w_{ss}(n) + \lambda w_{pp}(n))/\mu_n$, $n = 1, \dots, N+1$. Since $|u_n^*| = 1$, the proof is thus completed.

APPENDIX C

Denoting $a(n) = \cos(\angle(w_{ss}(n) + \lambda w_{pp}(n)) - \angle(w_{pp}(n)))$, γ_p can be rewritten as $\gamma_p(\lambda) = 2\sum_n |w_{pp}(n)| a(n) + d_{pp}$. Suppose that the values of $w_{ss}(n)$ and $w_{pp}(n)$ are given by $x_1 + jy_1$ and $x_2 + jy_2$, respectively, $x_1, x_2, y_1, y_2 \in \mathbb{R}$, then $a(n)$ can be expressed as

$$a(n) = \sqrt{1 - (x_2 y_1 - x_1 y_2)^2 / (a_1^2 + a_2^2 + a_3^2 + a_4^2)},$$

where $a_1 = (x_1 x_2 + \lambda x_2^2)$, $a_2 = (y_1 y_2 + \lambda y_2^2)$, $a_3 = (x_2 y_1 + \lambda x_2 y_2)$ and $a_4 = (x_1 y_2 + \lambda x_1 y_2)$. Since $\angle(w_{ss}(n)) \neq \angle(w_{pp}(n))$, i.e. $x_2 y_1 \neq x_1 y_2$, $\forall \lambda > 0$, $a(n)$ strictly increases as λ increases, which thus completes the proof.

REFERENCES

- [1] Q. Wu and R. Zhang, "Towards smart and reconfigurable environment: Intelligent reflecting surface aided wireless network," *IEEE Commun. Mag.*, vol. 58, no. 1, pp. 106–112, Jan. 2020.
- [2] C. Huang, A. Zappone, M. Debbah, and C. Yuen, "Achievable rate maximization by passive intelligent mirrors," in *Proc. IEEE ICASSP*, Apr. 2018, pp. 3714–3718.

- [3] Q. Wu and R. Zhang, "Intelligent reflecting surface enhanced wireless network via joint active and passive beamforming," *IEEE Trans. Wireless Commun.*, vol. 18, no. 11, pp. 5394–5409, Nov. 2019.
- [4] C. Huang *et al.*, "Holographic MIMO surfaces for 6G wireless networks: Opportunities, challenges, and trends," 2019. [Online]. Available: <https://arxiv.org/abs/1911.12296>.
- [5] Q. Wu and R. Zhang, "Beamforming optimization for wireless network aided by intelligent reflecting surface with discrete phase shifts," *IEEE Trans. Commun.*, Dec. 2019, DOI: 10.1109/TCOMM.2019.2958916.
- [6] S. Zhang and R. Zhang, "Capacity characterization for intelligent reflecting surface aided mimo communication," 2019.
- [7] Y. Yang, B. Zheng, S. Zhang, and R. Zhang, "Intelligent reflecting surface meets OFDM: Protocol design and rate maximization," 2019. [Online]. Available: <https://arxiv.org/abs/1906.09956>.
- [8] H. Li, R. Liu, M. Li, and Q. Liu, "IRS-enhanced wideband MU-MISO-OFDM communication systems." [Online]. Available: <https://arxiv.org/abs/1909.11314>.
- [9] Q. Wu and R. Zhang, "Weighted sum power maximization for intelligent reflecting surface aided SWIPT," *IEEE Wireless Commun. Lett.*, Dec. 2019, DOI: 10.1109/LWC.2019.2961656.
- [10] C. Pan *et al.*, "Intelligent reflecting surface enhanced MIMO broadcasting for simultaneous wireless information and power transfer." [Online]. Available: <http://arxiv.org/abs/1909.03272>
- [11] X. Guan, Q. Wu, and R. Zhang, "Intelligent reflecting surface assisted secrecy communication: Is artificial noise helpful or not?" *IEEE Wireless Commun. Lett.*, Jan. 2020, DOI: 10.1109/LWC.2020.2969629.
- [12] X. Yu, D. Xu, and R. Schober, "Enabling secure wireless communications via intelligent reflecting surfaces," 2019. [Online]. Available: <https://arxiv.org/abs/1904.09573>.
- [13] M. Cui, G. Zhang, and R. Zhang, "Secure wireless communication via intelligent reflecting surface," *IEEE Wireless Commun. Lett.*, vol. 8, no. 5, pp. 1410–1414, Oct. 2019.
- [14] H. Shen, W. Xu, S. Gong, Z. He, and C. Zhao, "Secrecy rate maximization for intelligent reflecting surface assisted multi-antenna communications," *IEEE Commun. Lett.*, vol. 23, no. 9, pp. 1488–1492, Sep. 2019.
- [15] Z. Ding and H. V. Poor, "A simple design of IRS-NOMA transmission," 2019. [Online]. Available: <https://arxiv.org/abs/1907.09918>
- [16] G. Yang, X. Xu, and Y.-C. Liang, "Intelligent reflecting surface assisted non-orthogonal multiple access," 2019. [Online]. Available: <https://arxiv.org/abs/1907.03133>.
- [17] X. Mu, Y. Liu, L. Guo, J. Lin, and N. Al-Dhahir, "Exploiting intelligent reflecting surfaces in multi-antenna aided NOMA systems." [Online]. Available: <https://arxiv.org/abs/1910.13636>
- [18] R. Zhang, Y.-C. Liang, and S. Cui, "Dynamic resource allocation in cognitive radio networks," *IEEE Signal Process. Mag.*, vol. 27, no. 3, pp. 102–114, May 2010.
- [19] J. Song, P. Babu, and D. P. Palomar, "Optimization methods for designing sequences with low autocorrelation sidelobes," *IEEE Trans. Signal Process.*, vol. 63, no. 15, pp. 3998–4009, Aug. 2015.